

**LOW-TEMPERATURE LOW-DOSE NEUTRON IRRADIATION EFFECTS ON  
BRUSH WELLMAN S65-C AND KAWECKI BERYLCO P0 BERYLLIUM —**  
L. L. Snead (Oak Ridge National Laboratory)

**OBJECTIVE**

This paper presents a summary of the results studying the effects of neutron irradiation to ITER-grade Brush Wellman S65-C beryllium and Kaweck Berylco P0 beryllium.

**SUMMARY**

The mechanical property results for two high quality beryllium materials subjected to low temperature, low dose neutron irradiation in water moderated reactors are presented. Materials chosen were the S65-C ITER candidate material produced by Brush Wellman, and Kaweck Berylco Industries P0 beryllium. Both materials were processed by vacuum hot pressing. Mini sheet tensile and thermal diffusivity specimens were irradiated in the temperature range of ~100-275°C from a fast ( $E > 0.1$  MeV) neutron dose of 0.05 to  $1.0 \times 10^{25}$  n/m<sup>2</sup> in the High Flux Isotope Reactor (HFIR) at the Oak Ridge National Laboratory and the High Flux Beam Reactor (HFBR) at the Brookhaven National Laboratory. As expected from earlier work on beryllium, both materials underwent significant embrittlement with corresponding reduction in ductility and increased strength. Both thermal diffusivity and volumetric expansion were measured and found to be negligible in this temperature and fluence range. Of significance from this work is that while both materials rapidly embrittle at these ITER relevant irradiation conditions, some ductility (>1-2%) remains, which contrasts with a body of earlier work including recent work on the Brush-Wellman S65-C material irradiated to slightly higher neutron fluence.

**PROGRESS AND STATUS**

**Introduction**

Beryllium has been considered for nuclear fuel cladding, nuclear fuel compacts and as a neutron moderator for fission power plants dating back to the early 1950's. Other than the non-structural application as a core moderator/reflector, this material has found little use in nuclear applications due to its low ductility.

The limited ductility of the various types of beryllium is a function of many factors including temperature, chemical purity, grain size and to some extent the rate at which the material is strained. Moreover, the hexagonally close packed beryllium crystal itself is resistant to slip severely limiting ductility potential of the material. The beryllium hcp crystal has only two operating slip modes (at least at low temperatures) being basal slip (0001) and prismatic slip (1010). For a high quality, high purity material, the ductility can be categorized into three temperature dependent regimes. In the low temperature regime ( $T < 200^\circ\text{C}$ ) the shear stress required to activate prismatic slip is quite high and failure typically occurs by cleavage of the basal plane. Total elongation in this temperature range for a high quality, vacuum hot pressed material (specifically Brush Wellman S65-C at 150°C) is ~5% in the direction parallel to the pressing direction and ~20% in the transverse direction. As the temperature is increased above this lower temperature regime the critical stress for prismatic slip decreases and both slip modes combine to yield peak total elongations of about 50% both parallel and transverse to the forming direction. In this intermediate temperature regime (~200-500) the failure is primarily ductile/fibrous tearing. As the temperature is further increased intergranular failure begins to occur returning the total elongation to below 20%.

Irradiation of beryllium with high energy neutrons has the effect of producing small loops or "black spots" at low temperatures ( $<400^{\circ}\text{C}$ )[1-5] with helium, formed by beryllium interaction with fast neutrons, forming bubbles from  $325\text{-}400^{\circ}\text{C}$ [6,7] and higher. The helium tends to form at grain boundaries from  $325\text{-}600^{\circ}\text{C}$ [7-15] and is also reported to be on dislocations within grains in the temperature range of  $450\text{-}550^{\circ}\text{C}$ . [7,8] Because the upper temperature of this study is  $\sim 50^{\circ}\text{C}$  less than the lowest temperature at which helium bubbles have been observed, the helium is thought to be in solid solution, though it is conceivable that bubbles too small to be easily resolved using transmission electron microscopy are present.

Both point defect clusters and helium bubbles adversely effect the mechanical properties of beryllium, regardless of its metallurgical form. Point defect clusters and bubbles tend to block dislocation motion resulting in a severe reduction in elongation and increased strength [1-3,10-13,16-21] and hardness [8,9,14,17,20,22]. The irradiation effects database has been reviewed in the past [7,17] mainly including work conducted prior to 1970.

## **Materials, Irradiation and Experimental Techniques**

### **Materials**

Table 1 lists the mechanical properties and impurity levels in the two materials chosen for this study. The first materials listed is an ITER first wall candidate beryllium, Brush Wellman S65-C. This material is vacuum hot pressed from impact ground Be powder ( $11\text{-}45\ \mu\text{m}$ ) at  $\sim 1050\text{-}1150^{\circ}\text{C}$  followed by a  $870^{\circ}\text{C}$  heat treatment to remove aluminum from solution by forming  $\text{AlFeBe}_2$  precipitates. The S65-C beryllium was provided by Brush Wellman (BW) and designated as process Lot 4880 and is a commercially available, high quality structural beryllium. The grain size of the final product was  $\sim 9\ \mu\text{m}$ . The second material chosen for this study was manufactured by the now defunct Kawecki Berylco Industries (KBI) and is designated as P0 (P-zero) taken from a billet No. 040. This material was manufactured (circa 1975) by vacuum hot pressing impact ground powder ( $\sim 9\ \mu\text{m}$ ) at a temperature of  $1065^{\circ}\text{C}$ . The grain size of the final product was  $\sim 2.9\ \mu\text{m}$ . This was a research grade material processed for reduced impurity content by doubly electrolytically refining the beryllium powder.

From Table 1 significant difference are seen in both mechanical properties and chemical composition for the two materials chosen. The strength (at least in the longitudinal direction) is greater for the KBI-P0 material as compared with the BW S65-C, while the fracture elongation is somewhat higher for the BW-S65-C. It is interesting to note that, while the KBI-P0 billets of material had very good ductility at the time of their manufacture, the elevated amount of BeO as compared with the BW S65-C (3.36 -vs.- 0.64 w%), and possible other metallurgical improvements, yields lower elongation than the present day commercial BW S65-C beryllium.

Samples were machined of each material by Speedring, Inc. (Cullman, AL) to Brush Wellman specifications. Two sample geometries were fabricated: (1) SS-3 mini-sheet tensile specimens which are pin loaded sheet tensiles, and (2) 6 mm diameter, 4 mm thick cylinders.

### **Irradiation Exposures**

Two water moderated fission reactors were used for the specimen irradiation. The Hydraulic Tube facility at the High Flux Isotope Reactor (HFIR) at the Oak Ridge National Laboratory was used to study the effect of fluence range at a constant irradiation temperature. Mini-sheet tensile specimens and thermal diffusivity (6 mm) discs were loaded inside an aluminum holder which was welded inside a "rabbit" capsule. The capsules were then baked at  $200^{\circ}\text{C}$  and stored in the presence of hygroscopic media. The rabbit was welded shut in an ultra high purity (UHP) helium environment. Each rabbit was radiographed and underwent a QA procedure to ensure air or water was unable to penetrate the capsule. Sample temperature was achieved by gas-gap

Table 1. Properties of Beryllium Materials Provided by Manufacturer

	Brush Wellman S-65C	Kawecki Berylco P0
Yield Stress (MPa) - Long.	257	
-Trans.	265	530
Ultimate Stress (MPa) - Long.	381	
-Trans.	414	655
Fracture Elongation (%) - Long	3.5	
-Trans.	6.6	4.9
Density		
Impurities : (wt %) BeO	0.64	3.36
(wt %) C	0.038	0.173
(appm) Fe	670	1000
Al	230	120
Si	255	70
Mg	30	40
Zn	<10	NA
Ni	<20	95
Mn	<20	30
Cu	25	15
Ti	65	NA
Co	8	<5
N	120	NA
Cr	50	90

conduction of the nuclear heating between the sample holder and the rabbit body, both made of Type 6061-T6 aluminum. Rabbits were irradiated in the HT-3 position with a thermal and fast ( $E > 0.1$  MeV) neutron flux of  $2.2 \times 10^{19}$  and  $7.8 \times 10^{18}$  n/m<sup>2</sup>, respectively.[23] Fluences of irradiation were 0.05, 0.2 and  $1.0 \times 10^{25}$  n/m<sup>2</sup> ( $E > 0.1$  MeV) at a calculated irradiation temperature of 300°C.

The High Flux Beam Reactor (HFBR) at the Brookhaven National Laboratory was used to study the effects of varied irradiation temperature at a constant fluence. Two irradiation capsules were designed for insertion into the V-15 core thimble position. Each capsule consisted of separate gas-gapped subcapsules containing the samples. Variations in the sample temperature in the different subcapsules was achieved by varying the gas gap between the subcapsules and the inside of the external capsule, which was in contact with the core coolant water. The subcapsule bodies were electro-discharge machined from Type 6061-T6 aluminum. Each subcapsule typically contained 4 SS-3 tensile specimens. After the samples were loaded, a Type 304 stainless steel roll pin (a spring) was lightly hammered into place to ensure that the specimens were in good thermal contact with the subcapsule wall. Each subcapsule used one type-K thermocouple which monitored temperature throughout the irradiation.

All samples and capsule components (for both reactor irradiations) were ultrasonically cleaned in isopropyl alcohol and acetone prior to capsule assembly. After the HFBR capsule was assembled and the ~33 meter umbilical Type 8000 aluminum tubing was welded in place, the capsule was helium leak checked using a helium mass spectrometer. The capsule was then evacuated using an oil-free turbomolecular pump and back-filled with UHP helium to 15 psig. This procedure was repeated three times. Between the first and second evacuation cycles the capsule was baked out to 400°C under vacuum. After the final backfill to 15 psig the pressure was monitored continuously from time of assembly until the end of the irradiation. At no time did the capsule pressure reach atmospheric pressure before or during the irradiation. However, a small helium leak caused the capsule pressure to decrease during irradiation. This was corrected during irradiation by valving off the irradiation capsules, and then evacuating and back-filling the gas

handling manifolds with helium (which were not removed after capsule construction.) Once the manifold was purged and backfilled with UHP helium, the capsule was repressurized with helium to 15 psig.

At the time of these irradiations the HFBR was operating at 30 MW<sub>th</sub> power. Recently, Greenwood [24] has conducted a calculation on a single dosimetry sample near the center of the V-15 thimble. The fast neutron fluence in this case was approximately half the value which he previously measured. For this paper, the recent flux measurements are used. Also, based on Monte Carlo calculations it is assumed that the center 40 cm of 55 cm core is flux-invariant, therefore no flux gradient along the capsule (hence the samples) is expected. Each of the capsules were irradiated for an estimated fast ( $E > 0.1$  MeV) and thermal fluences of  $\sim 5 \pm 0.2 \times 10^{24}$  n/m<sup>2</sup> and  $2.3 \times 10^{24}$  n/m<sup>2</sup>, respectively. During irradiation, the temperature of the samples were recorded continuously. The temperature variation for two HFBR irradiations were always less than 12°C, most of which is accounted for by movement of the capsule to the center of the core during irradiation. Data presented in the results section represents the mean value with the error bars representing the range.

Based on calculations made (Gabriel [25]) and the revised spectra of the HFBR provided by Greenwood [24] the helium concentration and displacements per atom (dpa) for the various irradiations are listed in Table 2. Note that due to the relatively higher flux at the extreme end of the neutron spectrum, the HFBR V-15 spectrum produces a slightly higher He/dpa ratio than the HFIR HT position.

Table 2. Irradiation Conditions

	Thermal Fluence $\times 10^{25}$ n/m <sup>2</sup>	Fast Fluence $\times 10^{25}$ n/m <sup>2</sup> ( $E > 0.1$ MeV)*	Fast Fluence $\times 10^{25}$ n/m <sup>2</sup> ( $E > 1.0$ MeV)	dpa	He conc. (appm)	He/dpa
HFIR	0.14	0.05	0.026	0.04	10	250
	0.6	0.20	0.11	0.15	37	
	2.8	1.0	0.53	0.74	190	
HFBR	2.3	$5 \pm 0.5$	$2.1 \pm 0.2$	0.34	250	824

\* energy cut-off is listed as  $E > 0.11$  MeV for HFBR results [24]

### Experimental Techniques

The thermal diffusivity of the samples was measured by a custom built thermal flash (xenon laser) apparatus. Following the thermal flash on the front surface, the rear surface temperature was measured by the infrared signal and the diffusivity calculated following Clark and Taylor's analysis. [26] Density and thickness values corresponding to the unirradiated or irradiated condition were used for the unirradiated and irradiated measurements, respectively. For the thermal diffusivity calculations the density was calculated by dry weight and physical dimensions. The thermal diffusivity of every specimen was measured before and after irradiation.

The room temperature thermal conductivity (K) was calculated using the measured thermal diffusivity ( $\alpha$ ), measured density ( $\rho$ ), and the assumed specific heat ( $C_p$ ) as follows:

$$K = \alpha \rho C_p$$

The conversion from thermal diffusivity to thermal conductivity used the assumption that the specific heat remained unchanged with irradiation.

Density was determined for calculation of swelling by using a density gradient column according to ASTM D1505-85 utilizing chemical mixtures of trichloroethane and ethylene bromide and calibrated glass floats [27]. The linear density gradient of the column was 0.35 (mg/cm<sup>3</sup>)/cm

yielding an accuracy of relative density change of approximately 0.005%. Prior to dropping the samples in the density gradient column all specimens were etched in a mixture of hydrofluoric acid and ethyl alcohol and then dried. Visible etching and etch pits were observed.

Tensile testing was performed in load control digitally recording the cross head displacement. Elevated temperature testing was performed in static argon with the thermocouple in contact with the sample grips. Room temperature testing was in air. A temperature saturation of at least 15 minutes was used prior to applying tensile load. In both the unirradiated and irradiated condition the S65-C specimens were pin-loaded while the irradiated P0 specimens had to be shoulder loaded due to failure at the pin-holes. A cross head displacement rate  $0.001 \text{ s}^{-1}$  was applied for the SS-3 mini-sheet tensile specimens which have a  $\sim 0.76 \text{ cm}$  gage section. This displacement rate is approximately the same as that used in the recent European ITER beryllium irradiation program [28] though is about an order of magnitude higher than the value recommended by the Materials Advisory Board [29]. The effect of increasing strain rate in beryllium is to reduce the temperature at which beryllium moves from brittle to ductile failure. However, this temperature shift is expected to be small for the strain rate differences noted here [30,31], though the general effect of strain rate on failure mode does need to be further studied, especially for irradiated material.

A Buehler Micromet 3 microhardness testing machine was used at 500 g and 1 kg loads to measure the Vickers hardness. The two loads gave essentially the same hardness values and the 500 g loads are reported here. Specimens were prepared for hardness testing by wet sanding the surface (in oil) to a polished finish. Any potential effects of the surface polish affecting the hardness were dismissed by indenting unprepared and prepared surfaces of unirradiated material and noting that no difference in hardness was seen over a wide range of applied load.

## Results

### Swelling and Thermal Conductivity

The effect of irradiation to these doses and temperatures had essentially no effect on the thermal conductivity or density of the materials selected. The density of the S65-C beryllium was measured to be  $1.844 \text{ g/cc}$ , or 99.82 percent theoretical density (%td) while the density of the P0 beryllium was  $1.849$ , or 100.05 %td. The higher than theoretical density of the P0 material can be explained by the elevated level of BeO (3.36 w/% at  $\sim 3.0 \text{ g/cc}$  density) in this material, as seen in Table 1. Upon irradiation, swelling occurred in all materials, though the amount of swelling was very small. The largest swelling occurred for the HFIR material irradiated to  $1 \times 10^{25} \text{ n/m}^2$  at approximately  $300^\circ\text{C}$  yielding  $+0.027 \pm 0.005\%$  for the S65-C material and  $0.038 \pm 0.005\%$  for the P0 material. The swelling of the HFBR materials was less than this ( $\sim 0.02\%$ ) and no difference with respect to the irradiation temperature was observed. These swelling levels are consistent with the work of Gol'tsev and coworkers [7,32]. It is noted that the temperatures at which the materials were irradiated in this study were substantially below the lowest temperature at which helium bubbles have been observed [6,7] and is therefore in a region where point defect mobility and clustering is responsible for swelling.

The thermal conductivity of unirradiated S65-C beryllium was measured to be  $190 \pm 5 \text{ W/m-K}$ . This was found using the measured thermal diffusivity and assumed unirradiated density of  $1.844 \text{ g/cc}$  and specific heat of  $1.825 \text{ J/g-K}$ . In the case of the material irradiated to  $1 \times 10^{25} \text{ n/m}^2$  ( $E > 0.1 \text{ MeV}$ ) at  $\sim 300^\circ\text{C}$ , the thermal conductivity was within the experimental error of the unirradiated value. A significant reduction in thermal conductivity is not expected unless the material is irradiated in the temperature and flux range where helium bubble formation and swelling becomes pronounced.

### Hardness

The embrittlement of these beryllium materials as a function of dose and temperature is given in Figs. 1 and 2, respectively. The elevated level of BeO in the KBI-P0 material results in a higher initial hardness for this material as compared to the S65-C material. Specifically, the room temperature unirradiated Vickers hardness was measured to be  $228 \pm 3 \text{ Kg/mm}^2$  as compared to  $181 \pm 2 \text{ Kg/mm}^2$  for S65-C. Essentially no increase in hardness was observed a dose of  $0.05 \times 10^{25} \text{ n/m}^2$  ( $E > 0.1 \text{ MeV}$ ) for the P0 material while a marked increase was seen for both materials following  $0.2 \times 10^{25} \text{ n/m}^2$  ( $E > 0.1 \text{ MeV}$ ). As the fluence was further increased to  $1.0 \times 10^{25} \text{ n/m}^2$  ( $E > 0.1 \text{ MeV}$ ) the hardness of both materials substantially increased. As seen in Fig. 2, the dependence of hardness on irradiation temperature is significantly different for the two materials. The higher BeO content P0 material appears to have a weak dependence on irradiation temperature while the increased hardness (DH) for the S65-C appears to drop off with irradiation temperature from a DH-44  $\text{Kg/mm}^2$  following the  $110^\circ\text{C}$  irradiation to  $\sim 25 \text{ Kg/mm}^2$  for the  $237^\circ\text{C}$  irradiated material.

### Tensile Properties

The effects of the neutron irradiation induced embrittlement on the tensile properties of both types of beryllium are given in Figs. 3-8. These figures plot the tensile data as a function of irradiation temperature for a constant HFBR dose and as a function of HFIR dose at a constant irradiation temperature. The elongation specified is the total (fracture) elongation while the yield strength is defined at the 0.2% offset yield. Specific dpa and helium concentration limits are found in Table 2.

As seen in Figs. 3 and 4, the effect of the neutron induced embrittlement of the S65-C to a dose of  $0.2 \times 10^{25} \text{ n/m}^2$  is to increase the tensile strength and reduce the total elongation. In the irradiated condition both room temperature and  $300^\circ\text{C}$  tensile curves exhibited ductile failure with  $\sim 2\%$  and  $\sim 5\%$  total elongation at failure (compliance corrected), respectively. For the irradiation temperature range shown in Fig. 5, the yield strength at room temperature decreases with increasing irradiation temperature, while the total elongation increases slightly. Figure 6 shows the same samples as plotted in Fig. 5, though for irradiation temperature tests. The trend toward increasing total elongation is still apparent, though the tensile strength appears to increase between the  $106^\circ\text{C}$  and  $202^\circ\text{C}$  irradiations, and then to fall off slightly. It is noted that the data points in Figs. 3-8 represent single sample tests and as seen from the  $202^\circ\text{C}$  irradiation of Fig. 6 (and in Figs. 3 and 7), there is a fair scatter in the tensile data (in contrast with the hardness data (Figs. 1 and 2.)) It is clear the significant increase in hardness from the  $0.2$  to  $1.0 \times 10^{25} \text{ n/m}^2$  level, as well as recent tensile and fracture toughness data on S65-C material irradiated to higher doses[28] that the S65-C material will continue to embrittle as dose is increased and will eventually become completely brittle.

Figures 7 and 8 gives the tensile properties for the KBI P0 material irradiated as a function of dose in the HFIR. At equivalent doses of  $0.2 \times 10^{25} \text{ n/m}^2$ , the P0 and S65-C both undergo approximately 50 MPa increase in room temperature yield strength, though the P0 material appears to lose substantially more ductility to become near completely brittle by a dose of  $1.0 \times 10^{25} \text{ n/m}^2$  for both room temperature and irradiation temperature tests. It is noted that the S65-C material, both at room temperature and  $300^\circ\text{C}$ , has substantially higher unirradiated fracture elongation (Table 1.)

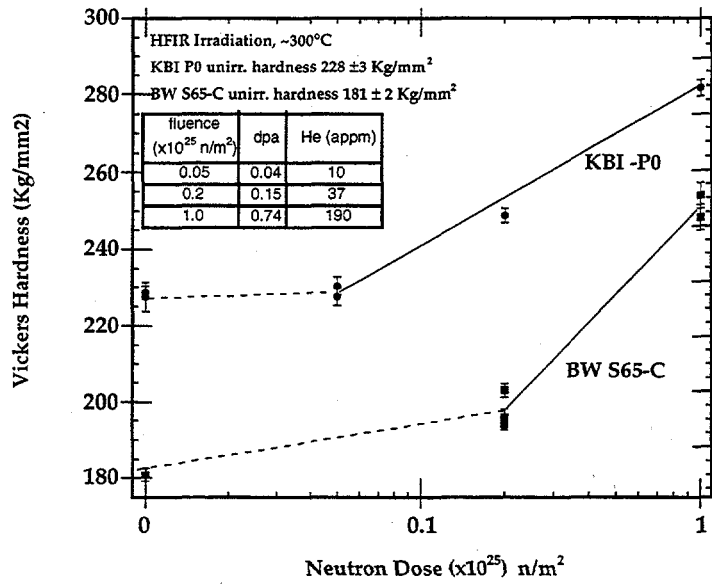


Figure 1. Hardness of BW S65-C and KBI P0 beryllium as a function of neutron dose.

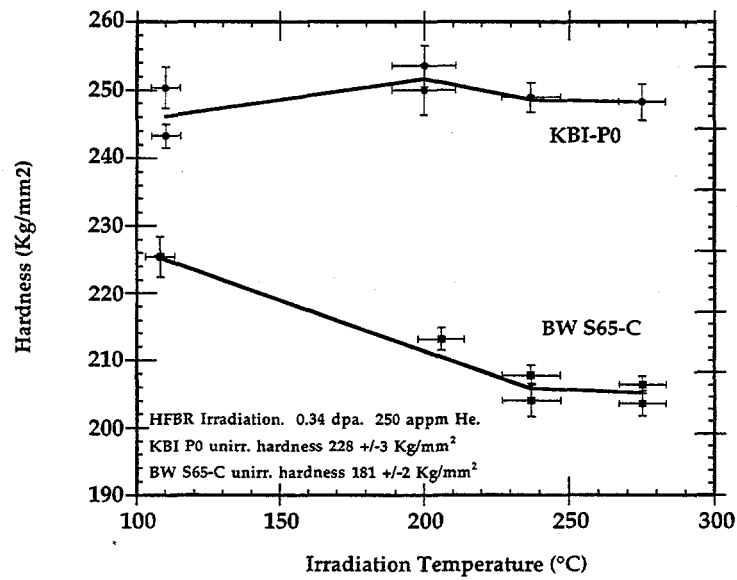


Figure 2 : Hardness of BW S65-C and KBI P0 beryllium as a function of irradiation temperature.

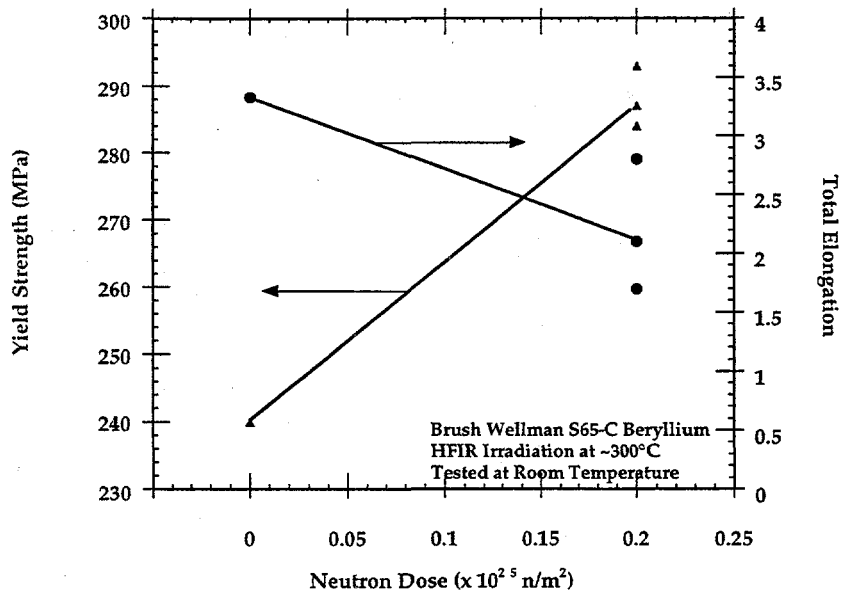


Figure 3: Room temperature yield strength and elongation of BW S65-C beryllium as a function of neutron dose.

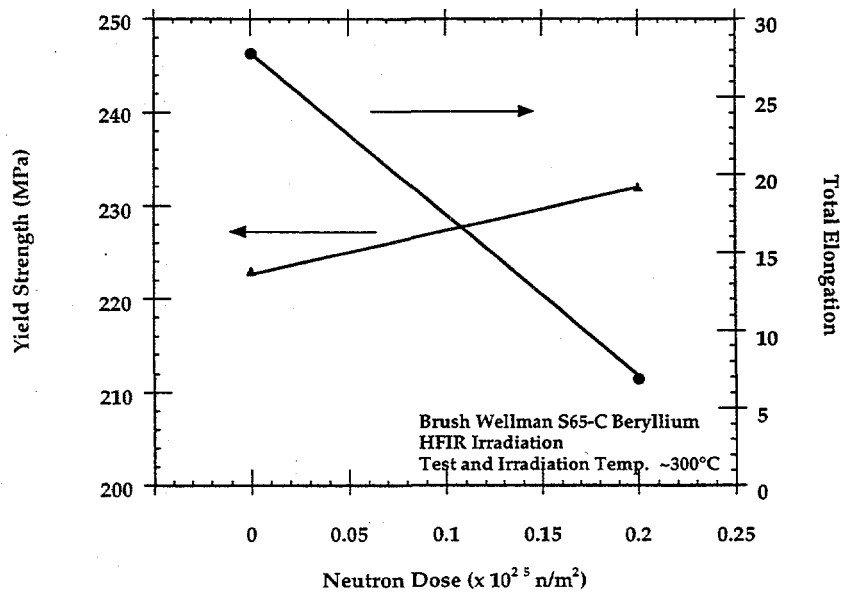


Figure 4: Yield strength and elongation of BW S65-C beryllium as a function of neutron dose measured at the irradiation temperature.

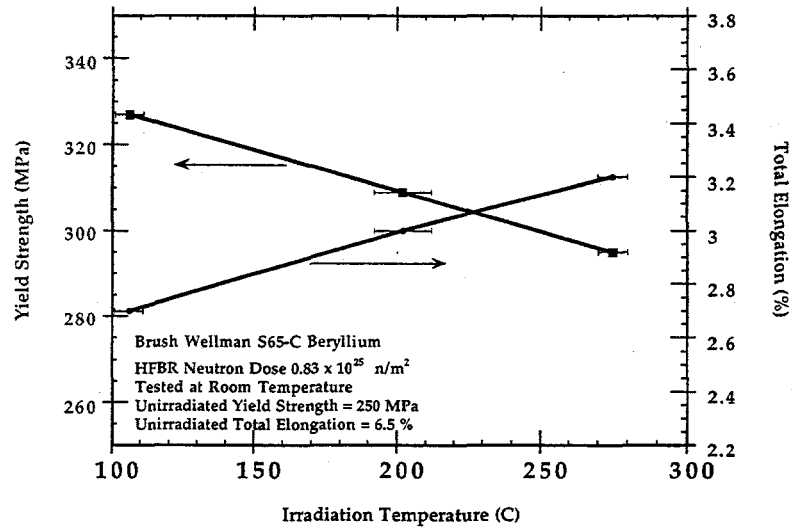


Figure 5 : Room temperature yield strength and elongation of neutron irradiated BW S65-C beryllium as a function of irradiation temperature.

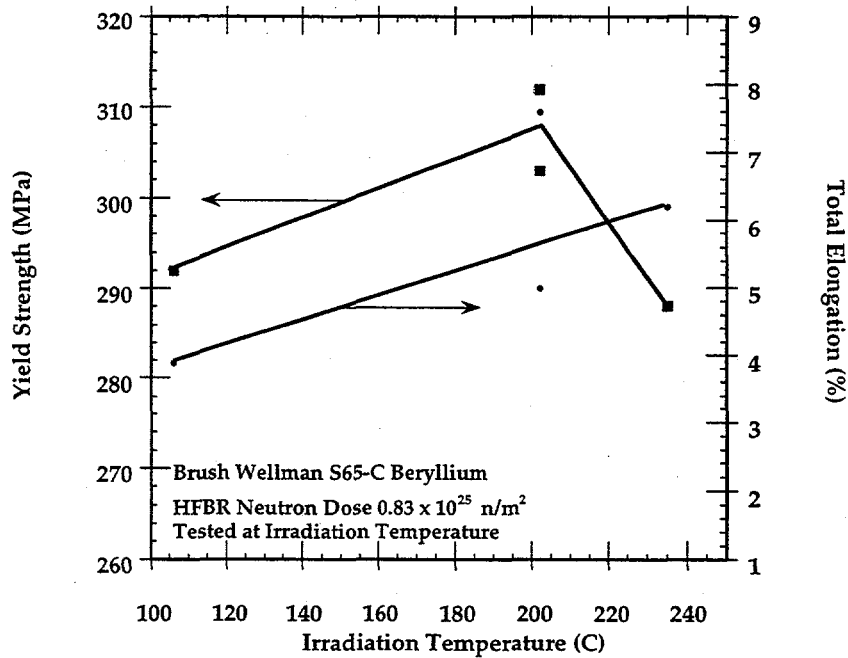


Figure 6 : Yield strength and elongation of neutron irradiated BW S65-C beryllium as a function of irradiation temperature measured at the irradiation temperature.

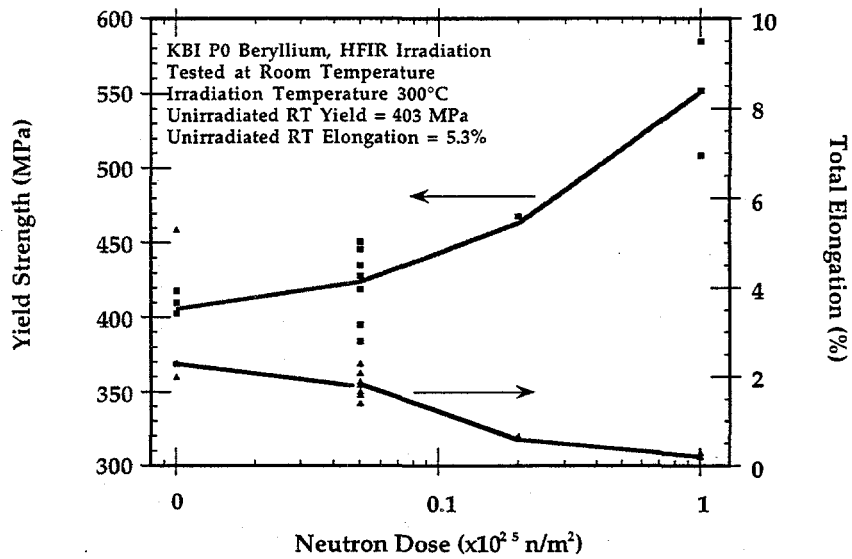


Figure 7 : Room temperature yield strength and elongation of KBI-P0 beryllium as a function of neutron dose.

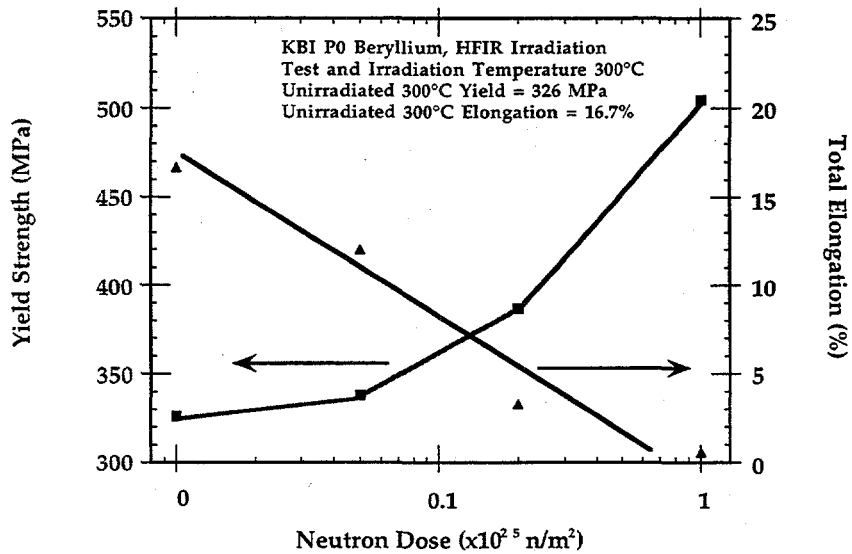


Figure 8 : Yield strength and elongation of KBI-P0 beryllium as a function of neutron dose measured at the irradiation temperature.

## ACKNOWLEDGMENTS

The author would like to thank Dave Dombrowski and the Brush Wellman company for provision of the S65-C material as well as for valuable technical assistance. I would also like to thank Ben Odegard of the Sandia National Laboratory for providing the materials and pertinent information regarding the Kawecki Berylco Industries P0 material. Technical help was also provided by J. P. Strizak, J. L. Bailey, and A. M. Williams for which I am grateful. Research sponsored by the Office of Fusion Energy Sciences, U.S. Department of Energy, under contract DE-AC05-96OR22464 with Lockheed Martin Energy Research Corp.

## REFERENCES

- [1] J.B. Rich and G.P. Walters, in *The Metallurgy of Beryllium* : Institute for Metals Monograph No. 28 (Chapman and Hall Ltd., London, 1961) p. 362.
- [2] J.M. Beeston et al., *Proc. Symp. on Materials Performance in Operating Nuclear Systems*, CONF-730801 , 1973) p. 59.
- [3] G.P. Walters, *J. Less Common Metals* 11 (1966) 77.
- [4] D.S. Gelles and H.L. Heinisch, *J. Nucl. Mater.* 191-194 (1992) 194.
- [5] R.S. Barnes, in *The Metallurgy of Beryllium*: Institute of Metals Monograph and Report Series No. 28 (Chapman and Hall, Ltd, London, 1961) p. 372.
- [6] J.M. Beeston, L.G. Miller, E.L. Wood-Jr and R.W. Moir, *J. Nucl. Mater.* 122-123 (1984) 802.
- [7] D.S. Gelles, G.A. Sernyaev, M.D. Donne and H. Kawamura, *J. Nucl. Mater.* 212-215 (1994) 29.
- [8] J.B. Rich, G.P. Walters and R.S. Barnes, *The Metallurgy of Beryllium* 4 (1961) 287.
- [9] B.S. Hickman et al., *Report UKAEA TRG Report 540* (1963).
- [10] B.S. Hickman and G. Bannister, *Report Part 2, AAEC/E-115* (also TRG Report 540 UKAEA) (1963).
- [11] G.T. Stevens and B.S. Hickman, *Report AAEC/E-133* (1965).
- [12] J.M. Beeston, in *Effects of Radiation on Structural Materials* vol. ASTM-STP 426 ((ASTM, Philadelphia, PA), 1967) p. 135.
- [13] E.D. Hyam and G. Sumner, *Radiation Damage in Solids*, vol. 1 (IAEA, Vienna, 1962) p. 323.
- [14] J.R. Weir, in *The Metallurgy of Beryllium* : Institute of Metals Monograph and Report Series No. 28 (Chapman and Hall, Ltd, London, 1961) p. 395.
- [15] R. Sumerling and E.D. Hyam, in *The Metallurgy of Beryllium* : Institute of Metals Monograph and Report Series No. 28 (Chapman and Hall, Ltd, London, 1961) p. 381.
- [16] E.H. Smith et al., *Proc. Symp. on the Physical Metallurgy of Beryllium*, Gatlinburg, CONF-730801 , 1973) p. 41.
- [17] J.M. Beeston, *Nucl. Eng. Des.* 14 (1970) 445.
- [18] J.M. Beeston, G.R. Longhurst, R.S. Wallace and A.P. Abeln, *J Nucl. Mater.* 195 (1992) 102.
- [19] M.H. Bartz, in *Properties of Reactor Materials*, Second United Nations Conf. on the Peaceful Uses of Atomic Energy vol. 5 (United Nations, Geneva, 1958) p. 466.
- [20] B.S. Hickman, in *The Metallurgy of Beryllium* : Institute of Metals Monograph and Report Series No. 28 (Chapman and Hall, Ltd, London, 1961) p. 410.
- [21] S. Morozumi, S. Goto and M. Kinno, *J. Nucl. Mater.* (1977) 82.
- [22] J.B. Rich, G.B. Redding and R.S. Barnes, *J. Nucl. Mater.* 1 (1961) 96.
- [23] S.T. Mahmood, S. Mirzadeh, K. Farrel and J.F. Pace, Oak Ridge National Laboratory, Oak Ridge Report ORNL/TM--12831 (1995).
- [24] L.R. Greenwood and R.T. Ratner, in *Fusion Materials Semiannual Progress Report for Period Ending Dec 31, 1997*. vol. DOE/ER-0313/23 , 1998) p. 309.
- [25] T.A. Gabriel, B.L. Bishop and F.W. Wiffen, Oak Ridge National Laboratory, Oak Ridge Report ORNL/TM-6361 (1979).
- [26] L.M. Clark and R.E. Taylor, *J. Appl. Phys* 46 (1975) 114.
- [27] ASTM, D1505-85, *Standard Test Method for Density of Plastics by Density Gradient Technique*, 1985.

- [28] R. Chaouadi, F. Moons and J.L. Puzzolante, SCK.CEN, Mol, Belgium Report TEC97/51/F040010/15/RC (1997).
- [29] Tests Methods Subcommittee Committee on Beryllium Metallurgy. National Academy of Sciences-National Research Council, Washington Report Publication MAB-205-M.
- [30] A.J. Martin and G.C. Ellis, in The Metallurgy of Beryllium : Institute of Metals Monograph and Report Series No. 28 (Chapman and Hall, Ltd, London, 1961) p. 3.
- [31] G.L. Turner, in Beryllium Science and Technology vol. 1, eds. D. Webster and G.J. London (Plenum Press, 1979) p. 145.
- [32] V.P. Gol'tsev, G.A. Sernyaev and Z.I. Chechetkina, Nauka i Teknika, Minsk (1977).